# Investigation on microstructure and mechanical properties on pulsed current gas tungsten arc welded super alloy 617

IOP Conf. Series: Materials Science and Engineering **263** (2017) 062032 doi:10.1088/1757-899X/263/6/062032

# Investigation on microstructure and mechanical properties on pulsed current gas tungsten arc welded super alloy 617

**K Mageshkumar[1,2], P Kuppan[2] and N Arivazhagan[2]**
[1] Ganadipathy Tulsis Jain Engineering College, Vellore - 632102, Tamil Nadu, India.
[2] School of Mechanical Engineering, VIT University, Vellore - 632014, Tamil Nadu, India.

E-mail: narivazhagan@vit.ac.in

**Abstract:** The present research work investigates the metallurgical and mechanical properties of weld joint fabricated by alloy 617 by pulsed current gas tungsten arc welding (PCGTAW) technique. Welding was done by ERNiCrCoMo-1 filler wire. Optical and Scanning Electron Microscope (SEM) revealed the fine equiaxed dendritic in the fusion zone. Electron Dispersive Spectroscopy (EDS) demonstrates the presence of Mo-rich secondary phases in the grain boundary regions. Tensile test shows improved mechanical properties compared to the continuous current mode. Bend test didn't indicate the presence of defects in the weldments.

## 1. Introduction

Alloy 617 is a solid solution strengthened nickel-based super alloy. The major alloying elements are chromium, cobalt, and molybdenum along with nickel matrix [1]. The alloying elements cobalt and molybdenum imparted by solid solution strengthening. The presence of small quantity of Ti and Al act as a precipitation strengthening. Alloy 617 is the workhorse material for the high-temperature applications, like gas turbine boiler tubes, combustion chambers and very high-temperature reactor [2, 3]. Alloy 617 is qualified material for section III of the ASME boiler and pressure vessel code for the very high-temperature reactor heat exchange application [4]. Alloy 617 has excellent mechanical property and creep resistance above 800$^{o}$C. Welding of alloy 617 in the above said applications plays a major role. Development of joining technique received paramount attention to the alloy 617. Welding of alloy 617 is possible by Gas Metal arc Welding(GMAW) process and Gas tungsten Arc welding(GTAW) process.

Alloy 617 is complicated with the formation of M23C6 carbide phases when it exposed to a high temperature between 650 – 750 oC. Wenjie et al. [1] compared the fusion zone microstructure of fiber laser, and CO2 laser of Inconel 617. The authors found the elemental segregation of Ti, Mo, Cr and Co in the interdendritic regions. Segregation of alloying elements Cr and Mo leads to the formation of M23C6 carbide phases. Mankins et al. [5]. Observed the formation of M23C6 phases in the grain boundary region when the alloy is aged at a different temperature between 649 to 1093oC for a long time between 215 to over 10,000h. The authors also reported that segregation of Mo and Cr largely responsible for the phase. A study by Arabi Jeshvaghani et al. [6]. indicated that precipitation of M23C6 phase in the interdendritic regions of alloy 617 due to the microsegregation of Cr and Mo at the end of the solidification. Lippold et al. [7] also identified the interdendritic (Cr, Mo)-rich eutectic

constituent in the fusion zone of Inconel 617 by the scheil-Gulliver simulations. Kimball et al. [8]. studied the heat treatment of alloy 617 temperatures between 593°C to 816°C for 168–8000 h. Authors found that continuous film of M23C6 carbide at the grain boundaries regions and the carbide denuded in the matrix near to grain boundary. Hirose et al. [9]. investigated the microstructure and mechanical properties of laser welded alloy 617. The authors observed the interdendritic gamma phases in the fusion zone. The presence of carbide phases leads to cracking in the grain boundary regions. This is due to the microsegregation of alloying elements.

The major issue associated with the joining of alloy 617 is susceptible to cracking in the grain boundary regions. Based on the foregoing, this can be achieved by preventing the formation of M23C6 phases during welding. This can be accomplished by reducing microsegregation of alloying elements during welding process by proper selection of welding process and parameters. In this context pulsed current gas tungsten arc welding shows some promise. It is a variation of continuous current gas tungsten arc welding. The present research being reported here deals with the investigation carried out to evaluate the current pulsing technique during GTA can be adopted to mitigate the problems of microsegregation in alloy 617 weldments.

Farahani et al. [10] carried out the comparative studies on alloy 617 by continuous and pulsed current gas tungsten arc welding of alloy 617. The authors reported a refined microstructure in the fusion zone with improved toughness in the weld joint compared to continuous GTA welding process. Comparative studies on GTAW and PCGTAW were also carried out by Ni-Cr-Mo based super alloy C-276 by Manikandan et al. [11, 12] the authors reported that joint fabricated by pulsed current gas tungsten arc welding shows improved mechanical properties with reduced microsegregation compared to continuous GTAW. The study reported by Janaki ram et al. [13] welding of alloy 718 by current pulsing technique reduced the unwanted laves phase in the fusion zone compared to GTAW.

## 2. Material and Methodology

The base metal used in the present study was alloy 617. The material was procured in the solution annealed condition in the form of 5mm thick plate. The chemical composition of as received base metal alloy 617 and filler wire are summarized in Table 1. The plates (170 mm x 55 mm x 5 mm) were cut with the help of EDM process. The plates were cleaned with acetone to remove dirt like oil contamination and other particles. Process parameters were finalized by a bead on trials. The optimized parameters are listed in Table 2. Standard Butt joint welding was carried out in PCGTA modes using KEMPI DWE 400 machine.

**Table 1.** Composition (%Wt) of Base and Filler Metal

| Elements | Ni | Cr | Co | Mo | Mn | Si | C | Cu | Fe | Others |
|---|---|---|---|---|---|---|---|---|---|---|
| Inconel 617 | 53.83 | 22.86 | 11.0 | 8.59 | 0.088 | 0.112 | 0.051 | 0.020 | 1.43 | <0.0010(B),0.376(Ti), 1.11 (Al), <0.010 (S) |
| ERNiCrCoMo1 | Rem | 21.8 | 12.45 | 9.05 | 0.20 | 0.65 | 0.06 | 0.04 | 0.75 | 0.30 (Ti), 0.005(P), 1.25 (Al) , 0.001 (S) |

The welded plate is shown in the fig. 1. The macro examination was carried out to see the depth of penetration and defects in the fusion zone. Optical and scanning electron Microscope (SEM) analysis were conducted to evaluate the microstructural changes in the fusion and HAZ zones. Standard procedures were adapted to polish the specimen. To reveal the microstructure electrolytic etching was done using Oxalic Acid. Energy Dispersive Spectroscopy (EDS) analysis was carried out on the microstructure samples to evaluate the microsegregation of the alloying elements. Tensile test specimens were prepared as per ASTM E8 standard. Tensile specimens were extracted with an axis perpendicular to weld direction. Universal tensile Machine (INSTRON make 8801) was used to

evaluate the strength and ductility of the welded joints. Tensile test was done triplicate to ensure the reproducibility of the results.

**Table 2.** welding parameters

| Filler metal | Filler Dia. (mm) | Pass Number | Current (A) | Voltage (V) | Welding speed (mms−1) | Heat Input (J) |
|---|---|---|---|---|---|---|
| ERNiCrCoMo1 (PCGTA) | 1.6 | 1(Root)<br>2<br>3<br>4 | Peak 130<br>Base 65 | 9.4-10.4<br>9.7-10.3<br>9.9-11.0<br>9.9-11.1 | 2.36<br>2.30<br>1.26<br>1.33 | 1975.07 |

SEM Factography analyses were carried out to evaluate the mode of fractures in the tensile sample. Root and Face Bend tests were done to assess the ductility of the weld joints; the test was done in the maximum angle of 1800. Samples were prepared as per the ASTM E190 standard.

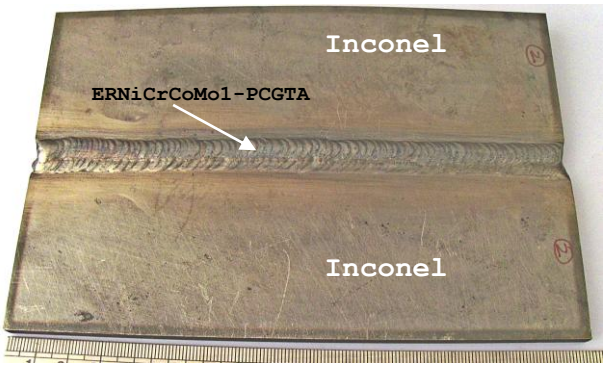


**Figure 1.** Photograph of Alloy 617 Weldment by PCGTA

## 3. Results and Discussions

*3.1. Weldment Quality*

Figure 2 illustrates the macrostructure of the weld joint fabricated by PCGTA with ERNiCrCoMo-1filler wire. The macro structure confirmed the defect free weld joints were obtained in PCGTA weldment.

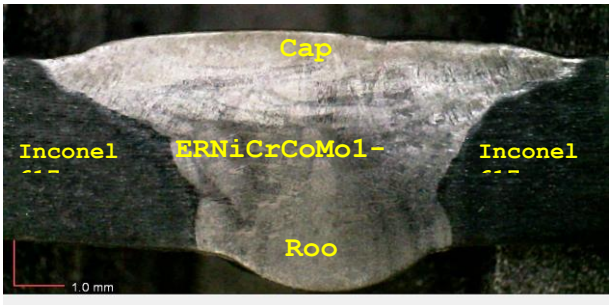


**Figure 2.** Macrostructure of Welded specimen using ERNiCrCoMo1

The macrograph indicated steady fluid flow in the weld pool and obtained the right welding morphology [11]. There is no problem in the lack of fusion and any other weldment defects. The macrostructure confined the process parameters employed in the present study is optimal.

*3.2 Microstructure Examination*

The alloy 617 was procured in the form of solution annealed and water quenched plate. Figure 3 represents the base metal microstructure of alloy 617. The microstructure consists of fine equiaxed grains. Twin boundaries were observed in the many of the austenitic matrix. Annealing twins originated during solution treatments. Twin boundaries can improve the strength by preventing the dislocation movement during deformation [10].

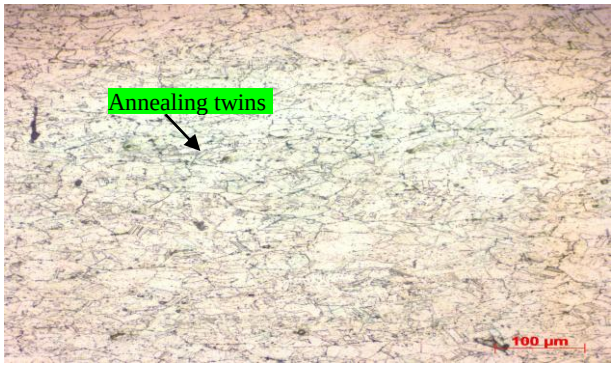


**Figure 3.** Microstructure of base metal alloy

The micrograph of the weld joint produced by PCGTA shown in fig.4. Figure 4a&b represents the weld interface and weld center, the fusion zone which consists of fine equiaxed dendritic structures. The weld interface shows the columnar dendritic structures. Grain coarsening was no seen in HAZ near to the fusion line. The presence of migration grain boundary (MGB) in the fusion zone.

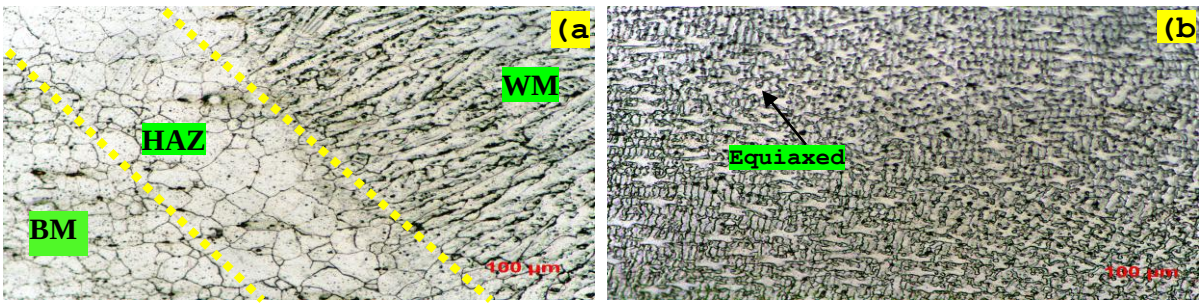


**Figure 4.** Microstructure of Inconel 617 weld plate by PCGTA using filler of ERNiCrCoMo1 weldment a) Weld interface b) Weld center

The results obtained from the optical microscope revealed that there is a refinement in microstructure. The PCGTAW welding shows the fine equiaxed dendritic structure. The migration grain boundaries were observed in the fusion zone. It may be attributed that the solute redistribution during solidification [14,15]. There is no evident in the presence of unmixed zone in the weldment. It can be attributed to the similarity of filler and base metal composition and the melting point temperature [16].

*3.3 SEM/EDS analysis*

The figures 5 represent the SEM/EDS analysis of PCGTA welded alloy 617 with ERNiCrCoMo-1. The micrograph shows the presence of secondary phases in the weldment. EDS analysis was carried out to evaluate the precipitates observed in the higher magnification SEM micrograph. EDS analysis confirmed the Mo-rich M6C carbide along with Cr –rich M23C6 phases at the interdendritic region of fusion zone center of weldment. Similar observation reported by Arabi et al. [17] and Lippold et al. [7] in the arc welding of alloy 617.

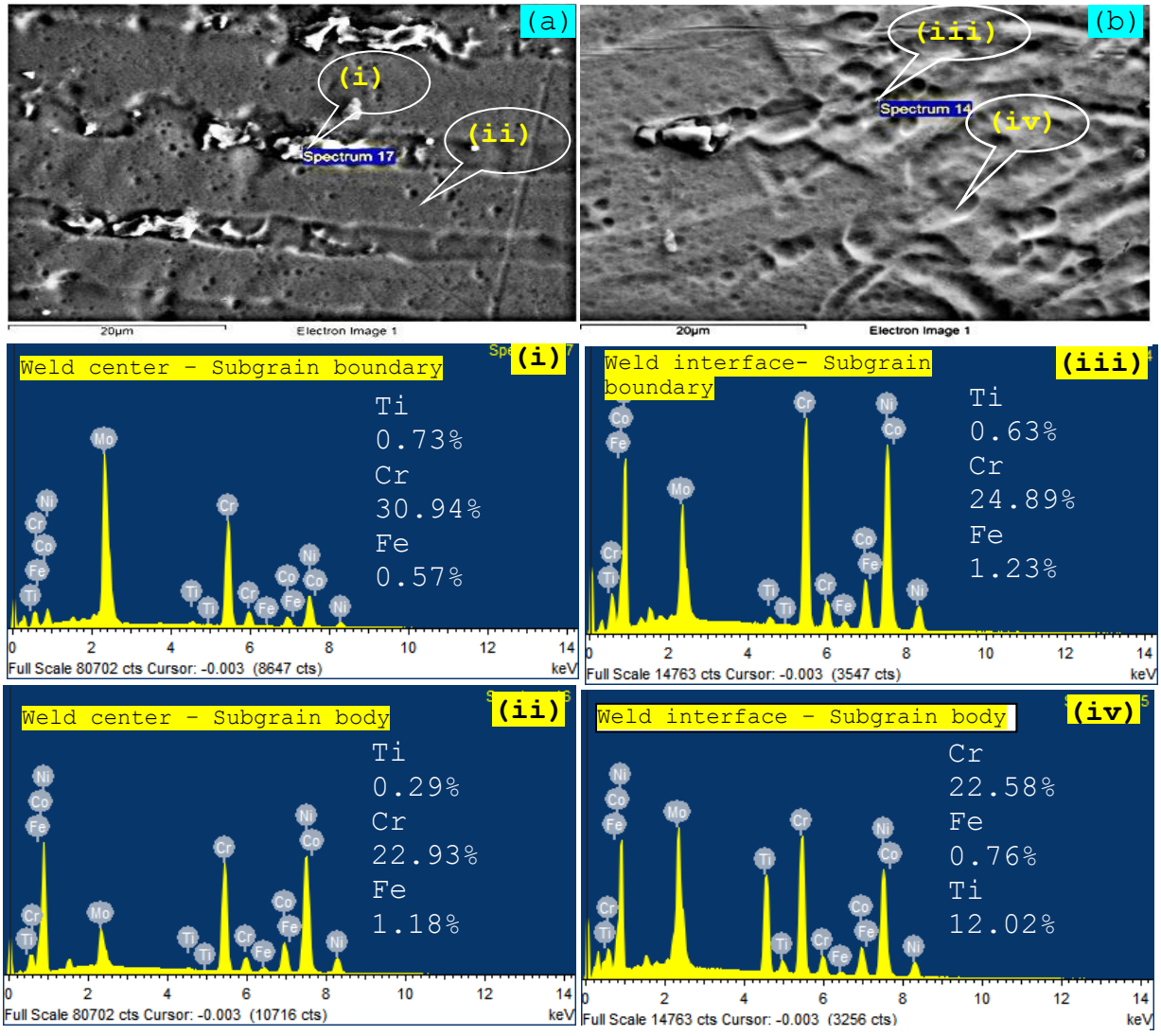


**Figure 5.** SEM/EDAX analysis of ERNiCrCoMo1-PCGTA welded plate of alloy 617 in various points of weldment a)SEM weld center b) SEM weld interface ,EDAX analysis of (i)Weld center subgrain boundary (ii) Weld center subgrain body (iii) Weld interface subgrain boundary and (iv) Weld interface subgrain body

*3.4 Mechanical Properties*

Table 3 listed the mechanical properties of the weld joint fabricated by PCGTA welding technique. Base metal properties also listed in the Table 3 for the comparison purpose. The strength of PCGTA is better than the base metal. The formation of M23C6 carbide phases noticed in the interdendritic region is largely responsible for the higher strength in the PCGTAW. The observed carbide phases in the interdendritic zone pinning with the grain boundary regions and it avoid the dislocation motions during deformation.

The higher SEM Fractography analysis was carried out to evaluate the mode of fracture in the tensile. It is observed from fractograph the crack was initiated in the interdendritic regions. The SEM micrograph Figure 7 shows the presence of microvoids with elongated dimples shows the ductile mode of fracture in both cases. Figure 8 shows the face and root bend test of PCGTAW. The photograph shows no evidence for the defect in the fusion zone. It confirmed that alloy 617 having good formability.

**Table 3**. Tensile test results

| Filler and base metal type | Yield strength (MPa) | Ultimate Tensile Strength (MPa) | Total elongation (%) | Location of Failure |
|---|---|---|---|---|
| ERNiCrCoMo1 (PCGTAW) | 327.37 | 828 | 13.08 | Weld Zone |
| Alloy 617 | 322 | 734 | 62 | - |

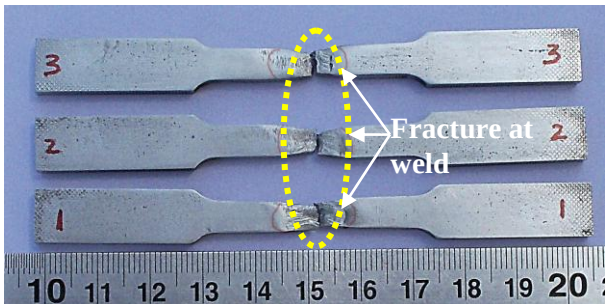


**Figure 6.** Photograph of failure tensile tested specimens

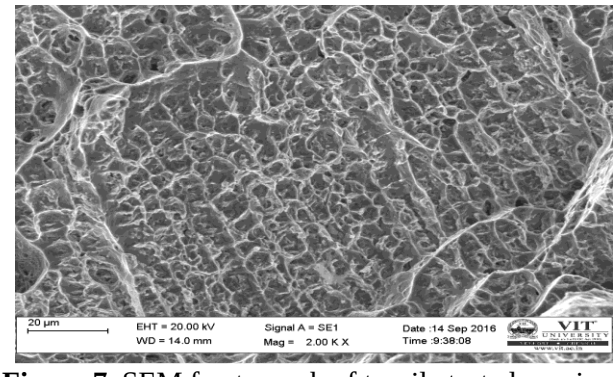


**Figure 7.** SEM fractograph of tensile tested specimen

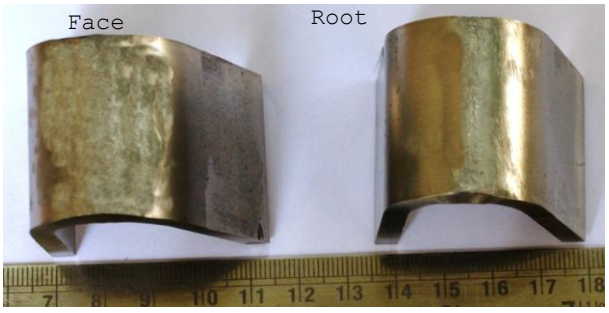


**Figure 8.** Bend Test of welded plate by PCGTA using filler of ERNiCrCoMo1

## 4. Conclusions

The following results obtained from the present study are listed.

- Macro examination confirmed the defect free welding was achieved in the optimized process parameter.
- The faster cooling rate achieved in the PCGTAW shows the refined microstructure and narrow HAZ in the fusion zone.
- SEM/EDS shows the presence of M23C6 carbide phase in the interdendritic regions. The presence of carbide phases improved the strength by reducing the dislocation motion during deformation
- Bend test didn't show the presence of any crack or other defects in the fusion zone.

## 5. References

[1] Ren, W. et al., 2015. A comparative study on fiber laser and CO2 laser welding of Inconel 617. Materials & Design, **76** 207–214
[2] J. Wang, J.X. Dong, M.C. Zhang, et al., Equilibrium-phase precipitation behaviors of typical nickel-base alloys for 700 ?C, J. Univ. Sci. Technol. B **34(7)** (2012) 799–807.
[3] W.L. Mankins, J.C. Hosier, T.H. Bassford, Microstructure and phase of INCONEL alloy 617 stability, Mater. Trans. 5 (1974) 2579–2590
[4] Ren, W., Drive, A. & Ridge, O., 2009. A Review on Current Status of Alloys 617 and 230 for Gen IV Nuclear Reactor Internals and Heat Exchangers. , **131(2)** 1–15
[5] Mankins, W. L., Hosier, J. C., and Bassford, T. H., 1974, "Microstructure and Phase Stability of INCONEL Alloy 617," Metall. Trans., **5** 2579–2590
[6] Arabi Jeshvaghani R, Harati E, Shamanian M. Effects of surface alloying on microstructure and wear behavior of ductile iron surface-modified with a nickel-based alloy using shielded metal arc welding. Mater Des 2011 **32** 1531–36
[7] L. John, BÖ Thomas, E. Carl, Cross (Eds.), Hot Cracking Phenomena in Welds II, Springer, Berlin, 2008 147–170
[8] Kimball, G. F., Lai, G. Y., and Reynolds, G. H., 1976, "Effects of Thermal Aging on Microstructural and Mechanical Properties of a Commercial Ni-Cr- Co-Mo Alloy Inconel 617," Metall. Trans. A, **7A**, 1951–1952
[9] A. Hirose, K. Sakata, and K.F. Kobayashi: Int. J. Mater. Product Technol., 1998, **13** 28-44
[10] Farahani, E., Shamanian, M. & Ashrafizadeh, F., 2012. A Comparative Study on Direct and Pulsed Current Gas Tungsten Arc Welding of Alloy 617., **2(1)** 1–6
[11] Manikandan, M. et al., 2014. Improvement of Microstructure and Mechanical Behavior of Gas Tungsten Arc Weldments of Alloy C-276 by Current Pulsing. Acta Metallurgica Sinica (English Letters), **28(2)** 208–215
[12] Manikandan, M. et al., Microstructure and mechanical properties of alloy C-276 weldments fabricated by continuous and pulsed current gas tungsten arc welding techniques. Manufacturing Processes **16** (2014) 563–572.
[13] Janaki Ram, G.D. et al., 2004. Control of Laves phase in Inconel 718 GTA welds with current pulsing. Science and Technology of Welding and Joining, **9(5)** 390–398.
[14] Sireesha M, Albert SK, Shankar V, Sundaresan S. A comparative evaluation of welding consumables for dissimilar welds between 316LN austenitic stainless steel and alloy 800. J Nucl Mater 2000;279:65–76
[15] Lippold JC, Koteki DJ. Welding metallurgy and weldability of stainless steels. John Wiley & Sons Inc; 2005

[16] Shah Hosseini, H., Shamanian, M. & Kermanpur, A., 2011.Characterization of microstructures and mechanical properties of Inconel 617/310 stainless steel dissimilar welds. Materials Characterization, **62(4)** 425–431.
[17] R. Arabi Jeshvaghani, M. Jaberzadeh, H. Zohdi, Microstructural study and wear behavior of ductile iron surface alloyed by Inconel 617, Mater. Des. **54** (2014) 491–497.